J Mater Sci (2007) 42:2974–2981
DOI 10.1007/s10853-006-0548-z

Direct measurement of the kinetics of geopolymerisation by in-situ energy dispersive X-ray diffractometry

John L. Provis · Jannie S. J. van Deventer

Received: 5 September 2005 / Accepted: 8 June 2006 / Published online: 9 December 2006
© Springer Science+Business Media, LLC 2006

Abstract In-situ energy dispersive X-ray diffractometry (EDXRD) using synchrotron radiation has been used to directly observe the kinetics of formation of a geopolymeric gel from a metakaolin precursor. The use of a purpose-built hydrothermal cell with polychromatic radiation from a wiggler source enables collection of a full diffraction pattern approximately every 150 s. This provides sufficient time resolution to observe the collapse of the metakaolin structure as it dissolves in the activating solution, accompanied by the reprecipitation of the geopolymeric gel binder phase from the now-supersaturated solution. Measurements taken on a limited set of samples of different composition (Si/Al ratio) show a clear trend in the rate of reaction with composition, and also a distinctly different mechanism of reaction in the most highly alkaline systems compared to those containing higher levels of dissolved silica in the activating solution. This corresponds to the results of previous microscopic observations showing significantly different microstructures in these systems, and confirms the value of this technique in analysis of the kinetics of geopolymerisation.

Introduction

One of the primary advantages of geopolymers over traditional cementitious materials is that correctly-formulated geopolymers are capable of very rapid setting while still attaining high final strengths [1]. The desire to understand and control this setting behaviour has led to the application of a variety of techniques in the analysis of the early stages of geopolymerisation. In particular, calorimetric [2, 3] and rheological [1, 4, 5] characterisation techniques have provided valuable information regarding the setting process. However, it is difficult to isolate the relative contributions of different steps in the reaction process to the total calorimetric signal, although work in this area is ongoing [6], and rheological studies are very difficult once the system has begun to solidify. Environmental scanning electron microscopy (ESEM) has also been used for in situ studies of geopolymerisation [7], but generally provides a more qualitative view of the process. Ex-situ X-ray diffraction (XRD) studies of geopolymeric 'hydroceramic' materials cured at slightly elevated temperature have used the degree of crystalline zeolite formation as a measure of the extent of reaction [8]. However, this technique provides unsatisfactorily low time resolution and relies on the formation of XRD-detectable crystallites, which are not always present in detectable quantities in geopolymers, particularly at higher Si/Al ratios [9]. It is therefore desirable to develop a technique by which structure development in a setting geopolymer may be directly observed, particularly in terms of isolating the dissolution and reprecipitation steps involved in the geopolymerisation process [10].

The use of in-situ energy-dispersive X-ray diffractometry (EDXRD) using a polychromatic X-ray source and an energy-discriminating detector for rapid obtention of diffractograms was first suggested in the late 1960s [11]. However, this technique has only

J. L. Provis · J. S. J. van Deventer (✉)
Department of Chemical and Biomolecular Engineering, The University of Melbourne, Melbourne, VIC 3010, Australia
e-mail: jannie@unimelb.edu.au

recently become more widely utilised, with recent improvements in synchrotron X-ray sources and detectors providing greatly improved signal-to-noise ratios [12–14]. Where the standard (angle-dispersive) XRD technique uses a monochromatic beam and a detector that scans through a range of angles, the polychromatic ('white') X-ray beam used in EDXRD allows the energy-discriminating detector to be fixed at a given angle. In Bragg's Law, Eq. (1), the diffracted beams from structures with different d-spacings are distinguished by different values of λ for a fixed θ, rather than the different values of θ observed in standard XRD (using fixed λ).

$$n\lambda = 2d\sin\theta \quad (1)$$

EDXRD has been used particularly in the investigation of hydrothermal reaction processes, which require sample vessels capable of withstanding relatively aggressive environments [15–17]. The higher penetrating power of the white X-ray beam used in EDXRD compared to a beam that has passed through a crystal monochromator (required for standard, angle-dispersive XRD experiments) enables the use of 'laboratory-sized' sample cells in transmission geometry, thereby greatly simplifying experimental design and expanding the available parameter space. The removal of the need to scan the detector across a range of angles also greatly decreases the collection time required to obtain a diffractogram. Some spatial resolution is sacrificed due to the difficulties inherent in energy-discriminating detectors, meaning that diffraction data obtained by EDXRD is most likely unsuitable for use in a structure refinement, but the temporal resolution achievable more than compensates for this.

The primary purpose of this investigation is to outline the value of EDXRD as a technique for the study of the kinetics of geopolymerisation. A series of potassium aluminosilicate geopolymers of varying Si/Al ratio are synthesised within a purpose-designed sample cell, and the reaction kinetics observed by EDXRD. It is shown that EDXRD provides sufficient time resolution to distinguish certain important features of the reaction process, and therefore provides a valuable complement to more established techniques.

Experimental details

In-situ reaction cell setup

Experiments were conducted at beamline X17C of the National Synchrotron Light Source (NSLS), Brookhaven National Laboratory, NY [18, 19]. This is a superconducting wiggler beamline, providing sufficient X-ray flux for experiments to be conducted in transmission geometry using a relatively large (approx. $2cm^3$, thickness 12 mm) sample. The beam size was 25×12 μm. A purpose-built sample vessel, constructed from stainless steel with a thin PTFE insert and end caps to contain the sample as shown in Fig. 1, was mounted on a kinematic stage and inserted into the beamline.

Temperature control in the reaction cell was achieved via the heating loop depicted in Fig. 1, with water from a temperature-controlled bath circulated by a small pump through channels drilled in the stainless steel block. The reaction cell temperature was able to be controlled to within approximately ± 3 °C (at 40 °C) using this system. The time taken to reach the desired reaction temperature (40 °C) following filling of the cell with geopolymer paste and connection of the heating system was less than the time taken to mount the cell on the kinematic stage and carry out the required safety procedures prior to the start of data collection. Therefore, temperature variation during start-up of the experiments is not considered in detail in this investigation, although it will be discussed later as a possible source of error.

X-ray detection and energy discrimination was achieved by the use of a solid-state Ge detector, located at a fixed 2θ angle of 8°, utilising a 0.3×1.0 mm brass collector and analysed through a 4000-channel MCA, spanning the energy range 3–74 keV. Calibration was carried out using a polycrystalline gold standard. The volume sampled by the X-ray beam was much smaller than the actual geopolymer paste volume, which meant that exact sample alignment was much less critical than in most beamline-based experiments. This was essential in ensuring the shortest possible start-up time for each experiment, allowing the maximum possible amount of data to be collected in the early stages of reaction. The 3D kinematic stage was set in the appropriate position, which remained constant throughout the series of experimental runs. Once the sample chamber was filled and the temperature control system attached, the vessel was mounted on the stage using a G-clamp. Measurements taken using a dummy sample with the kinematic stage located in a variety of different positions (much wider than the variability allowed in the start-up procedure for the actual experiments) all produced identical results. Therefore, any slight variations in sample position due to the abbreviated sample alignment procedure will not have any effect on the results obtained.

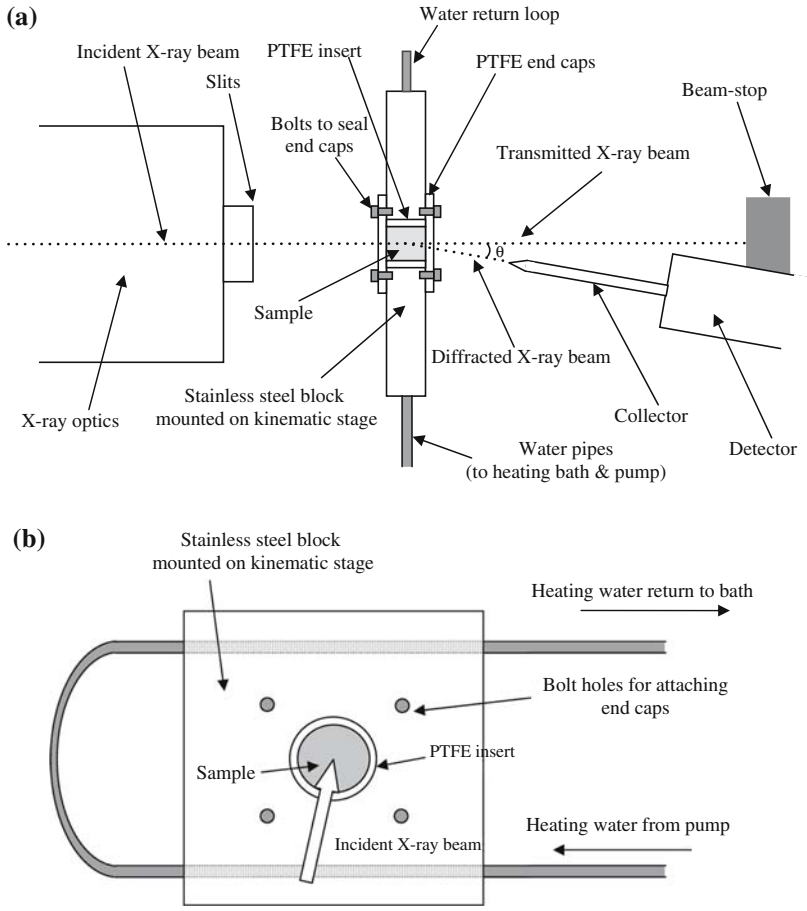

Fig. 1 Schematic diagrams of the experimental apparatus: (**a**) top cutaway view, not to scale, (**b**) front view of reaction cell with PTFE end cap removed

Geopolymer paste formulation

Potassium silicate solutions were prepared by dissolving amorphous silica in KOH solution with $H_2O/K_2O = 11.0$, giving solutions with composition $SiO_2/K_2O = 0.0$, 1.0, and 2.0. These solutions were then each mixed with stoichiometric amounts of metakaolin (MetaMax EF, Engelhard, NJ, USA, $SiO_2/Al_2O_3 = 2.0$) using a high-speed mechanical mixer to give smooth geopolymer pastes with $K_2O/Al_2O_3 = 1.0$ and SiO_2/Al_2O_3 ratios of 2.0, 3.0 and 4.0 respectively. A quantity of the paste was then transferred to the reaction cell, which was sealed, attached to the heating system and mounted on the kinematic stage in the beamline. The time taken from the start of mixing to the start of data collection was recorded for each experimental run, and was always in the range 7–9 min. The exact time taken to load the sample was dependent on the SiO_2/K_2O ratio of the geopolymer, as the higher-SiO_2 activating solutions are very viscous and therefore require more mixing time to produce a homogeneous geopolymer paste.

Notes on data collection and processing

In selecting the collection time per data set for an in situ EDXRD experiment, a compromise must be drawn between maximising the signal to noise ratio of each data set (energy resolution) and maximising the number of data sets collected (temporal resolution). Given that the main purpose of this investigation was the study of the kinetics of geopolymerisation, and that metakaolin-based geopolymers generally show no sharp diffraction peaks [9], a collection time of approximately 150 s was selected as being appropriate. Use of a collection time this short allows the obtention of a sufficient number of data points in the early stages of reaction. The spectrum obtained at each point in time was then smoothed by averaging over blocks of seven adjacent energy channels, which significantly reduced the noise in the data without sacrificing any valuable information due to the very broad nature of all peaks being observed. Figure 2 shows a comparison between the raw and smoothed data sets obtained after 60 min of reaction for the sample with $SiO_2/Al_2O_3 = 3.0$.

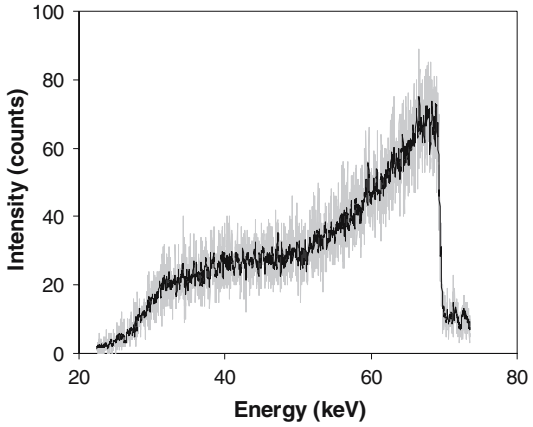

Fig. 2 Effects of smoothing over seven adjacent energy channels: Spectrum obtained from sample with $SiO_2/Al_2O_3 = 3.0$ after 60 min of reaction at 40 °C, raw (gray line) and smoothed (black line)

For the purposes of comparison between data sets, all values used in quantitative analysis are normalised by dividing by the total intensity (area under the curve). This is necessary due to fluctuations in beam intensity during a kinetic run, and removes the need to correct separately for detector deadtime effects.

The EDXRD experiments were conducted until no change could be detected between several successive data sets, and this was designated the point at which reaction was deemed to be effectively complete as measurable by this technique. While it is known that the reactions involved in geopolymerisation do actually continue for many hours past the point of setting, as shown by heat capacity data from modulated DSC [20], it is not practical to carry out beamline experiments over this very extended period of time. EDXRD data sets were obtained for fully cured (>7 days) geopolymer samples, which showed some differences when compared to the 'final' data sets from the kinetic runs. However, attempts to use the fully cured samples as an endpoint for data quantification (see Section Quantification of the degree of reaction) were unsuccessful. A possible reason for this is that the initial solid phase that forms in a geopolymer system is in fact transformed to a slightly different phase following the initial setting process [21, 22], and therefore comparison of intermediate data sets with this second phase will not give useful information regarding the kinetics of the initial setting process and formation of the first solid phase. The 'extent of reaction' as discussed throughout this paper is in fact referring only to the formation of this initial solid phase—the longer timescales required for the second phase to form are not accessible by in situ beamline techniques.

Results and discussion

Features of the data sets

Figures 3–5 show smoothed and normalised data sets for the geopolymerisation of pastes with $SiO_2/Al_2O_3 = 2.0$, 3.0 and 4.0 respectively. Each data set was collected over a 150 s period.

Figures 3–5 show a superficially similar trend in reaction progress across compositions. Each set of diffractograms shows a large feature at high energy (~68 keV) in the initial stages of the reaction, which gradually diminishes and is replaced by a broad peak at ~30–50 keV as the reaction progresses. It is not yet entirely clear which structural features of the geopolymerising paste are responsible for these features, particularly given that the high-energy peak corresponds to a d-spacing of around 1.3 Å, which is significantly shorter than the T–O bond length (~1.6 Å, T: tetrahedral Si or Al). However, it is possible that this peak is at least partially due to scattering from small dissolved species, which would explain why its relative intensity decreases with the solidification of the reacting paste.

The peak at ~30–50 keV falls approximately in the region that, by Bragg's law, corresponds to d-spacings of 1.8–3.0 Å. This compares to an expected T–O bond length of 1.6–1.8 Å—at the lower end of this range for Si–O, and at the higher end for Al–O [23]. This peak becomes noticeably more intense throughout

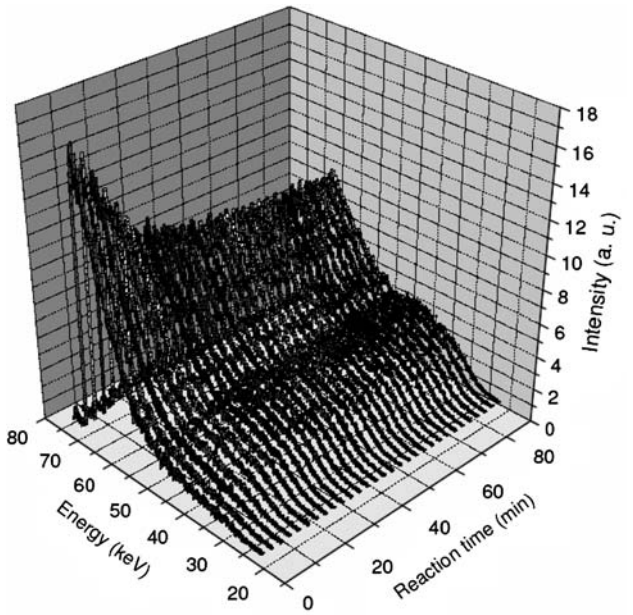

Fig. 3 Smoothed and normalised EDXRD data for the system with $SiO_2/Al_2O_3 = 2.0$

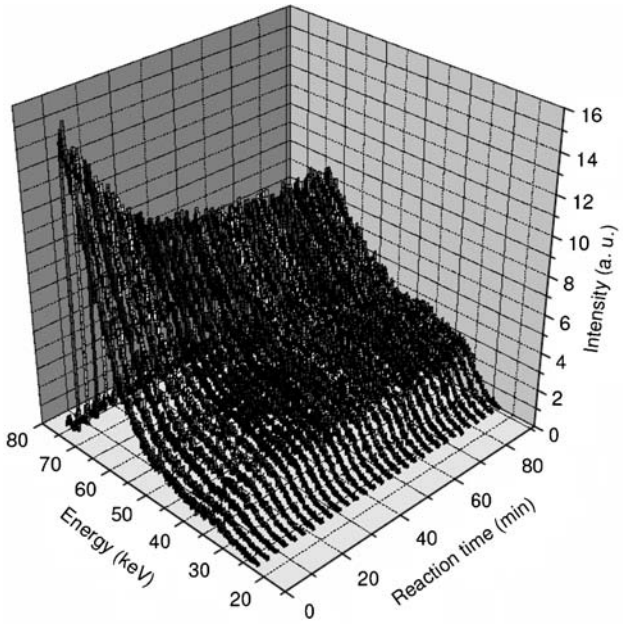

Fig. 4 Smoothed and normalised EDXRD data for the system with $SiO_2/Al_2O_3 = 3.0$

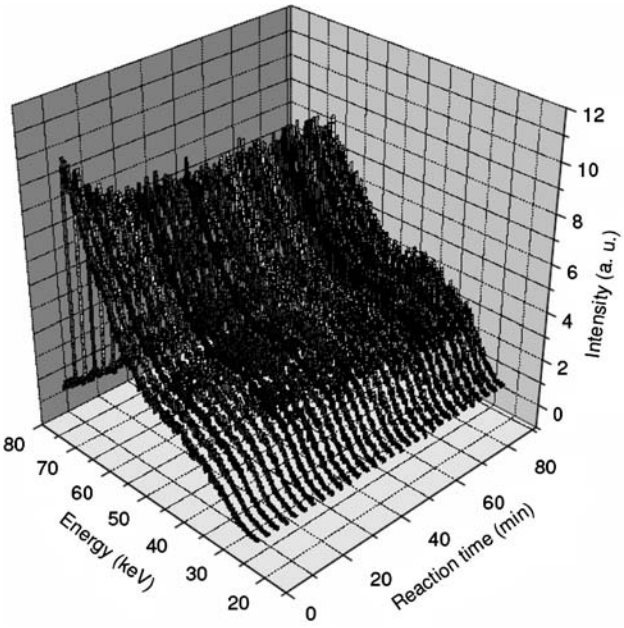

Fig. 5 Smoothed and normalised EDXRD data for the system with $SiO_2/Al_2O_3 = 4.0$

geopolymerisation, suggesting that the degree of structural ordering on this length scale is increasing as the reaction progresses. This may be related to the increasing uniformity in T–O–T bond lengths as the reaction progresses. Metakaolin contains a mixture of 4-, 5- and 6-coordinated Al [24], and each different coordination state will have a different Al–O bond length. As the metakaolin dissolves, all the Al is converted to 4-coordinated $Al(OH)_4^-$, which is the preferred state of Al in alkaline solution [25]. This coordination is then maintained during the incorporation of the dissolved Al into the geopolymer binder phase [26], meaning that the bond lengths in the geopolymer phase will be more uniform than those in the metakaolin. Also, the geopolymer phase is overwhelmingly comprised of Q^4 sites (i.e. T sites connected to four other T sites), meaning that the number of non-bridging oxygen atoms in a geopolymer phase is low [2, 27, 28], whereas the dissolved species will obviously contain many non-bridging oxygens, some of which are deprotonated. T–O bond lengths depend on whether the O is bridging or non-bridging [29, 30], and also on the protonation state of the oxygen atom. These non-uniformities are largely removed with the formation of the geopolymeric binder phase, which is expected to lead to a higher degree of ordering on this length scale as observed in Figs. 3–5.

The rapid decrease in spectral intensity below 30 keV is due to absorption effects. X-rays below this energy cannot pass through a sample and vessel endcaps as thick as those used here, rendering any effects at d-spacings greater than approximately 3.0 Å unobservable. The design of the X17C beamline and detector also do not allow the use of a smaller 2θ angle which would render longer d-spacings accessible. It is hoped that future work, possibly in further reducing the sample vessel size and endcap thickness to minimise absorption while maintaining the rapid initialisation capabilities of the current apparatus, will lead to improvements in this area.

Quantification of the degree of reaction

Quantification of the extent of reaction based on the data sets presented in Figs. 3–5 was achieved based on the simple assumption that each intermediate spectrum was able to be represented as a linear combination of the first and last spectra obtained. The data presented in Figs. 3–5 represent the time period from the start of reaction until the reaction had slowed sufficiently that no change was observable for several successive spectra. Once these data had been collected, a spectrum with a much longer (usually 2000s) collection time was obtained, to provide a 'final' reference point with the highest possible signal to noise ratio. As shown in Fig. 6, fitting each intermediate spectrum according to Eq. (2) by a least-squares error minimisation gave a respectably accurate fit to the spectra.

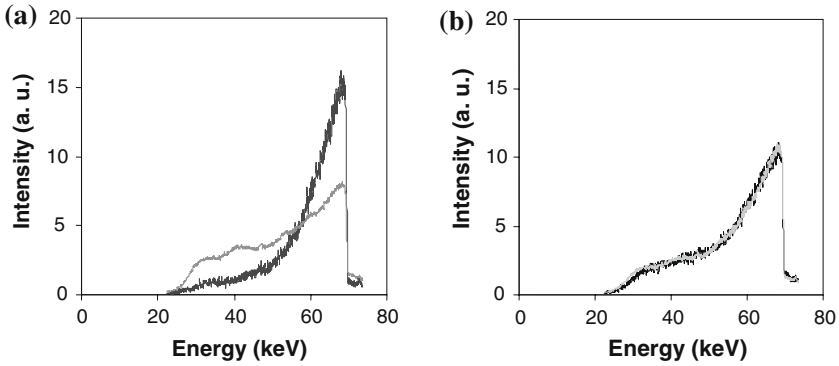

Fig. 6 EDXRD spectra of the system with $SiO_2/Al_2O_3 = 3.0$: (**a**) First and final spectra, obtained 8.33 min (black line) and 4 h 47 min (grey line) after the start of mixing respectively. (**b**) Spectrum obtained after 24.2 min (black line), with the fit obtained by linear combination of the spectra in Fig. 6(**a**) (grey line) with $x = 0.628$

$$(\text{Spectrum at time } t) = x(\text{Final spectrum}) + (1-x)(\text{Initial spectrum}) \quad (2)$$

However, it must be noted that the raw x values obtained by this procedure are not in fact a truly representative measure of the extent of reaction at any given point in time, due to the fact that the first data point could not be obtained at time $t = 0$. To remedy this, some means of estimating the extent of reaction during the period leading up to the obtention of the first spectrum is necessary. It was initially hoped that it would be possible to use the spectrum of unreacted metakaolin as a point of comparison to obtain this information. However, differences in X-ray absorption behaviour between metakaolin and the geopolymer pastes due to their different atomic compositions cause severe complications in this procedure. Therefore, a simpler method for estimating the rate of reaction in the initial stages of geopolymerisation was chosen. It was observed from the data sets presented as Figs. 3–5, as well as others not shown in this paper, that the extent of reaction in the early stages of geopolymerisation, to a first approximation, increases linearly. This observation was used to provide an estimate of the progress of the reaction in the time period leading up to collection of the first spectrum, and appears to give results that are reasonably accurate. Future work is intended to provide a better solution to this problem, both with respect to design of apparatus and experiments and also in numerical treatment of experimental data.

Having corrected the raw data obtained by spectral fitting using this assumption of linearity, Fig. 7 is obtained. This figure shows that the primary aim of this investigation, to develop an accurate means of quantifying the rate of the initial stages of geopolymerisation using EDXRD, has been achieved. The trend shown in Fig. 7, where the rate of reaction decreases with increasing SiO_2/Al_2O_3 ratio for samples of constant H_2O/K_2O ratio, corresponds to previous observations using calorimetric and rheological techniques [31, 32]. Figure 8 is a plot of reaction rate against time, calculated by numerical differentiation of the data presented in Fig. 7.

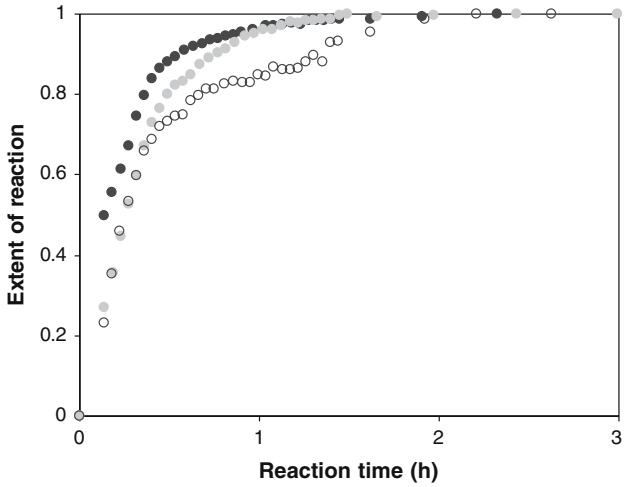

Fig. 7 Plot of extent of reaction vs. time for samples with $SiO_2/Al_2O_3 = 2.0$ (black circles), 3.0 (grey circles) and 4.0 (unfilled circles)

Figure 7 shows that increasing the SiO_2/Al_2O_3 ratio of a geopolymer paste reduces the rate of the initial burst of reaction prior to solidification of the paste. The data shown in Fig. 8 show that the use of a higher SiO_2/Al_2O_3 ratio also extends the length of time over which reaction occurs, although there is some scatter in this plot due to the difficulties inherent in numerical differentiation of experimental data.

Plotting data in the form shown in Fig. 8 also provides a means of qualitative comparison with the results of calorimetric (ICC or DSC) experiments. A direct quantitative comparison is not possible due to the effects of variations in the heats of reaction with composition in calorimetric experiments, as well as the presence of heat flow signals from other processes

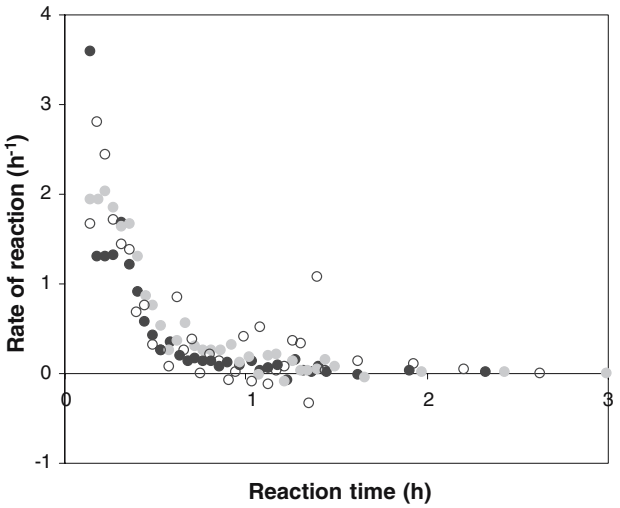

Fig. 8 Plot of rate of reaction vs. time for samples with SiO_2/Al_2O_3 = 2.0 (black circles), 3.0 (grey circles) and 4.0 (unfilled circles)

including rearrangements of dissolved species [6]. However, the reaction timescales observed in Fig. 8 are roughly consistent with preliminary DSC studies using the same brand of metakaolin, as well as with published data using a different metakaolin [33].

It is not currently possible to quantify the total proportion of metakaolin converted into geopolymeric binder by EDXRD. However, ^{27}Al MAS-NMR has shown that the total extent of conversion of metakaolin into geopolymer after curing for 2 weeks decreases with increasing SiO_2/Al_2O_3 ratio [26, 34]. The results presented here provide a potential explanation for this trend, in that the slow initial rate of reaction in very high-silica systems may mean that these pastes solidify before the dissolution of metakaolin reaches completion. The apparent 'step' in the SiO_2/Al_2O_3 = 4.0 data set in Fig. 7 after approximately 1 h of reaction provides further evidence for this suggestion, as it appears that the reaction becomes drastically slower at this point, which corresponds to a relative extent of reaction of around 0.8. Approximately 20% of the reaction observed occurs after this point in time, but it is likely that metakaolin dissolution will be greatly hindered by the reduced mobility of the dissolved species following solidification. Therefore, the lower overall extent of metakaolin conversion in these systems is not unexpected. This is in contrast to the lower-silica samples (SiO_2/Al_2O_3 = 2.0 and 3.0), where Fig. 7 shows that the reaction goes essentially to completion in the first 90 min after mixing, and Fig. 8 confirms this by displaying almost zero rate of reaction for these samples after this time.

Conclusions

Energy dispersive X-ray diffractometry, using a temperature-controlled sealed hydrothermal cell in transmission geometry on a superconducting wiggler synchrotron beamline, has been shown to be an effective technique in measuring the reaction kinetics during the initial setting period of the geopolymerisation reaction sequence. Fitting the smoothed and normalised spectra obtained at intermediate time points as linear combinations of the first and final spectra provides a remarkably accurate quantitative measure of the extent of reaction as it progresses towards completion. The rate of reaction in a geopolymer-forming paste is shown to decrease with increasing silica content when all other factors are held constant. Solidification of the paste prior to the completion of reaction in high-silica systems is observable, which corresponds to previously published NMR data.

Acknowledgements The experimental portion of this work was carried out on beamline X17C at the National Synchrotron Light Source, Brookhaven National Laboratory, which is supported by the U.S. Department of Energy under Contract No. DE AC02-98CH10886. Valuable technical assistance from Dr. Jingzhu Hu is gratefully acknowledged. This work was funded through the Particulate Fluids Processing Centre, a Special Research Centre of the Australian Research Council, and by an Australian-American Fulbright Postgraduate Scholarship awarded to JLP and hosted by the University of Illinois at Urbana-Champaign and the University of Delaware.

References

1. Lee WKW, Van Deventer JSJ (2002) Cem Conc Res 32:577
2. Rahier H, Van Mele B, Biesemans M, Wastiels J, Wu X (1996) J Mater Sci 31:71
3. Granizo ML, Blanco-Varela MT, Palomo A (2000) J Mater Sci 35:6309
4. Rahier H, Van Mele B, Wastiels J (1996) J Mater Sci 31:80
5. Phair JW, Smith JD, Van Deventer JSJ (2003) Mater Lett 57:4356
6. Provis JL, Duxson P, Van Deventer JSJ, Lukey GC, (2005) Chem Eng Res Des 83:853
7. Wei S, Zhang Y-S, Wei L, Liu Z-Y, (2004) Cem Conc Res 34:935
8. Olanrewaju J (2002) Ph.D. Thesis, Pennsylvania State University, 268 pp
9. Provis JL, Lukey GC, Van Deventer JSJ (2005) Chem Mater 17:3075
10. Van Jaarsveld JGS, Van Deventer JSJ, Lorenzen L (1997) Miner Eng 10:659
11. Giessen BC, Gordon GE (1968) Science 159:973
12. Cheetham AK, Mellot CF (1997) Chem. Mater. 9:2269
13. Morón MC (2000) J Mater Chem 10:2617
14. Walton RI, O'Hare D (2000) Chem Commun 2283
15. He H, Barnes P, Munn J, Turrillas X, Klinowski J (1992) Chem Phys Lett 196:267

16. Evans JSO, Francis RJ, O'Hare D, Price SJ, Clark SM, Flaherty J, Gordon J, Nield A, Tang CC (1995) Rev Sci Instrum 66:2442
17. Walton RI, Millange F, O'Hare D, Davies AT, Sankar G, Catlow CRA (2001) J Phys Chem B 105:83
18. Thomlinson W, Chapman D, Gmür N, Lazarz N (1988) Nucl Instr Meth Phys Res A 266:226
19. Decker G (1990) Nucl Instr Meth Phys Res A 291:357
20. Swier S, Van Assche G, Van Hemelrijck A, Rahier H, Verdonck E, Van Mele B (1998) J Therm Anal 54:585
21. Palomo A, Alonso S, Fernández-Jiménez A, Sobrados I, Sanz J (2004) J Am Ceram Soc 87:1141
22. Fernández-Jiménez A, Palomo A (2005) Micropor Mesopor Mater 86:207
23. Petkov V, Billinge SJL, Shastri SD, Himmel B (2000) Phys Rev Lett 85:3436
24. Rocha J, Klinowski J (1990) Angew Chem Int Ed Engl 29:553
25. Swaddle TW (2001) Coord Chem Rev 665:219
26. Duxson P, Lukey GC, Separovic F, Van Deventer JSJ (2005) Ind Eng Chem Res 44:832
27. Barbosa VFF, Mackenzie KJD, Thaumaturgo C (2000) Int J Inorg Mater 2:309
28. Duxson P, Provis JL, Lukey GC, Separovic F, Van Deventer JSJ (2005) Langmuir 21:3028
29. Kubicki JD, Sykes D (1995) Geochim Cosmochim Acta 59:4791
30. Pereira JCG, Catlow CRA, Price GD (1999) J Phys Chem A 103:3252
31. Rahier H, Simons W, Van Mele B, Biesemans M (1997) J Mater Sci 32:2237
32. Van Jaarsveld JGS, Van Deventer JSJ (1999) Ind Eng Chem Res 38:3932
33. Rahier H, Denayer JF, Van Mele B (2003) J Mater Sci 38:3131
34. Duxson P, Provis JL, Lukey GC, Mallicoat SW, Kriven WM, Van Deventer JSJ (2005) Colloid Surf A 269:47